

High resolution pre-stack seismic inversion using few-shot learning



Ting Chen^{*}, Yaojun Wang, Hanpeng Cai, Gang Yu, Guangmin Hu

University of Electronic Science and Technology of China, China

ARTICLE INFO

Keywords:

Few-shot learning
Artificial neural network
Seismic inversion

ABSTRACT

We propose to use a Few-Shot Learning (FSL) method for the pre-stack seismic inversion problem in obtaining a high resolution reservoir model from recorded seismic data. Recently, artificial neural network (ANN) demonstrates great advantages for seismic inversion because of its powerful feature extraction and parameter learning ability. Hence, ANN method could provide a high resolution inversion result that are critical for reservoir characterization. However, the ANN approach requires plenty of labeled samples for training in order to obtain a satisfactory result. For the common problem of scarce samples in the ANN seismic inversion, we create a novel pre-stack seismic inversion method that takes advantage of the FSL. The results of conventional inversion are used as the auxiliary dataset for ANN based on FSL, while the well log is regarded the scarce training dataset. According to the characteristics of seismic inversion (large amount and high dimensional), we construct an arch network (A-Net) architecture to implement this method. An example shows that this method can improve the accuracy and resolution of inversion results.

1. Introduction

High resolution pre-stack seismic inversion is a major technology for reservoir characterization (Zong et al., 2012). Due to the limitation of seismic data quality, it is difficult to obtain a high resolution reservoir parameter from seismic data (Alemie and Sacchi, 2011). Previous studies found that introducing prior information or reasonable rock physical model into the inversion framework can improve the resolution of inversion results (Hampson et al., 2005; She et al., 2019; de Figueiredo et al., 2019). However, the current methods need to design mathematical models satisfying different assumptions, they are only applicable to some specific scenarios, but difficult to complex geological areas.

The current research shows that ANN has powerful feature extraction and parameter learning ability, and the inversion methods combined with ANN are more efficient than conventional one. It has been used to obtain velocity model from the CSP gathers (Röth and Tarantola, 1994; Araya-Polo et al., 2018). A variant of ANN called recurrent neural network (RNN) has been used for full-waveform inversion (Richardson, 2018). Chen et al. (2019) applied iterative deep neural networks (DNN) to inverse seismic wavelet and reflectivity. To make network more perfect, the training process requires to have a sufficient amount of valid labeled data (Goodfellow et al., 2016; Dai et al., 2019). ANN has a huge development in the field of image, partly because it is easy to get valid

labeled data in this field, but it is very expensive to get in the field of geophysics. To alleviate the problem of scarce samples, adding constraints to the ANN inversion framework to improve network generalization ability has become the choice of many researchers. For example, the ANN framework with initial models as constraints (Zhang et al., 2021); A convolution neural network (CNN) employing a physics-guided approach and data drive (Biswas et al., 2019; Sun et al., 2021). Song et al. (2022) proposed an inversion framework based on semi-supervised learning. In this work, we employ another ANN learning architecture named FSL for high resolution pre-stack seismic inversion of reservoir parameters.

The ANN algorithms usually require hundreds or thousands of supervised samples to ensure generalization ability (Lu et al., 2020). The FSL is significant and challenging in the field of ANN. Due to the mature mathematical principle, conventional inversion method could integrate well log and seismic data in reasonable good manner. The results of conventional inversion are used to construct the auxiliary dataset, and a few of accurate well log is regarded as the scarce training dataset. In order to adapt to the characteristics of ANN seismic inversion with large amount data but few labeled samples, we create a new A-Net architecture to implement the method. This network firstly increases the number of the convolution kernel layer by layer to enlarge the feature quantity, and then reduces the number of the convolution kernel to extract high-dimensional features. FSL can still achieve a satisfactory result with

* Corresponding author.

E-mail address: ting.chen.seven@gmail.com (T. Chen).

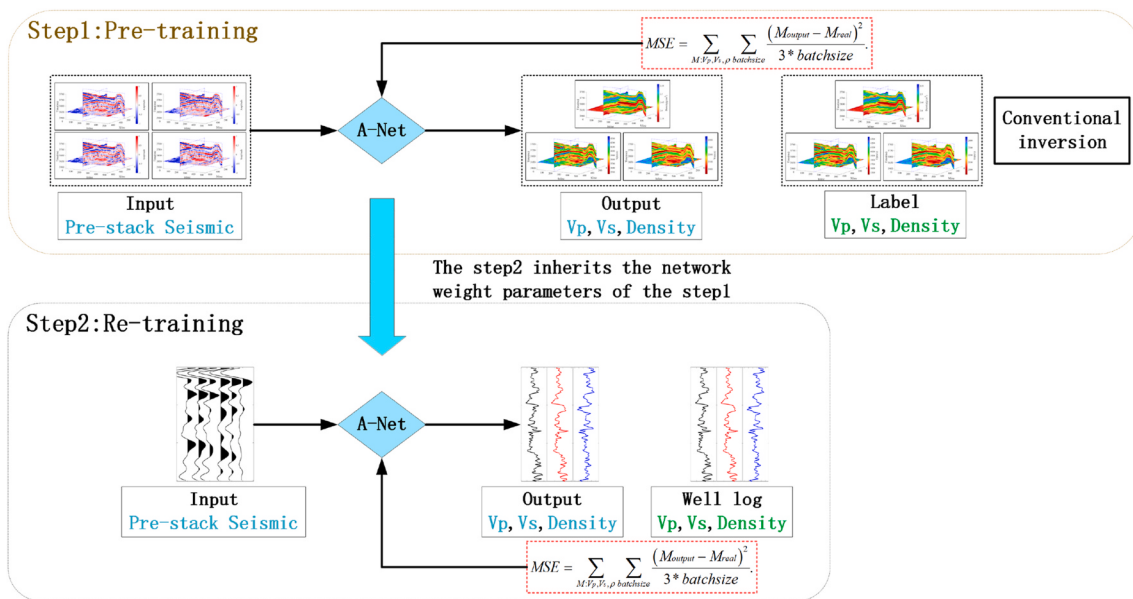


Fig. 1. The framework of the proposed method.

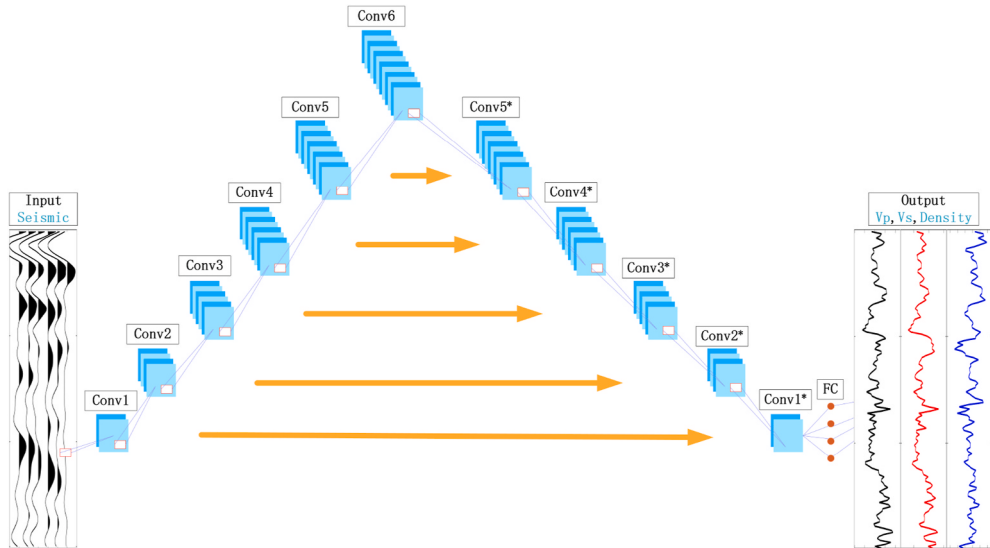


Fig. 2. A-Net architecture for pre-stack seismic inversion. The pre-stack seismic angle gathers is the input of the network and the reservoir parameters curve V_p , V_s and ρ is the output, that compare with prepared or true well log.

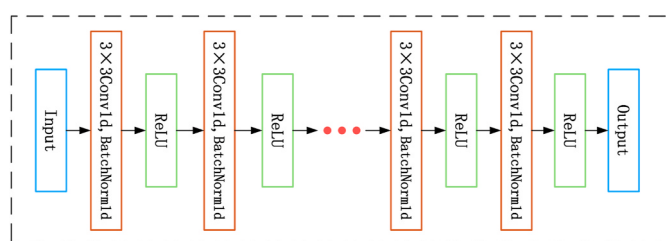


Fig. 3. The convolutional unit architecture. Input is the pre-stack seismic angle gathers or an output from a previous unit, and output is the input to the next unit.

few samples. This method is successfully applied to a filed data set from northwest of China by effectively improving the resolution of inversion results.

2. Method

The objective of training an ANN is to find an input-to-output mapping and minimize the error between the network output and the labels. The complicity of the structure and the number of valid data largely determine the predictive ability of supervised ANN (Das et al., 2019). ANN applies successfully in the field of image classification because it is easy to obtain valid labeled data (Krizhevsky et al., 2012), whereas in the geophysical inversion it is often difficult to obtain numerous valid labeled data. To meet this challenge, we combine the conventional pre-stack inversion with FSL to construct a new high resolution inversion method. The whole framework of the proposed method is shown in Fig. 1, and the two main parts are marked by dotted boxes.

2.1. Step 1: Pre-training for the original network

The results of conventional inversion are used for pre-training, and

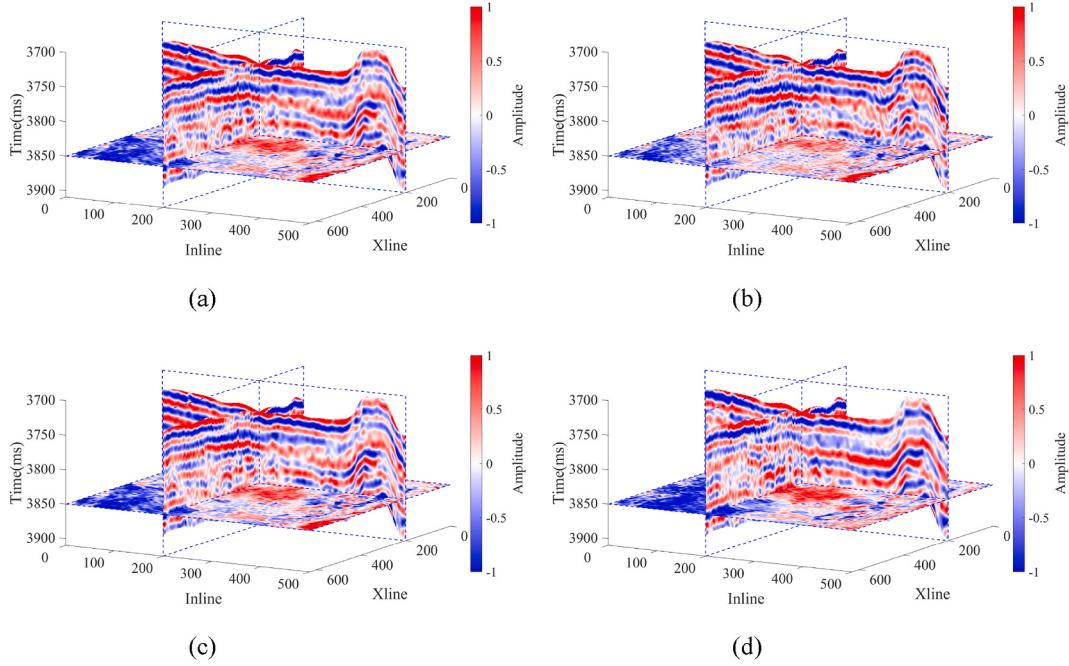


Fig. 4. Post-stack and pre-stack seismic via various angles. (a) post-stack seismic data set; (b) near angle-stack seismic data set; (c) middle angle-stack seismic data set; (d) far angle-stack seismic data set.

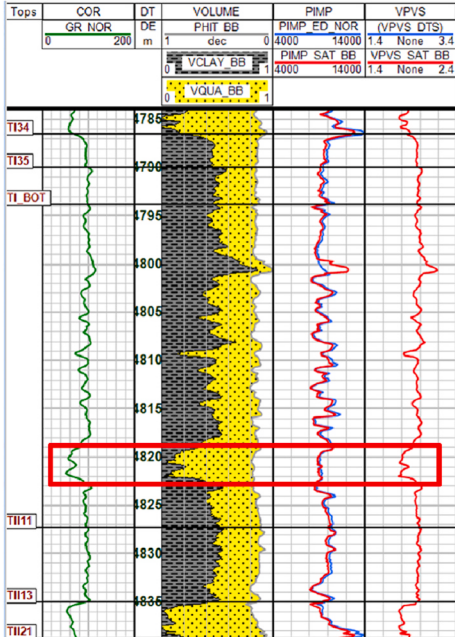


Fig. 5. Log analysis of well. The red rectangle in the plot is the location of the TII0 gas formation.

the hidden relationship between pre-stack seismic data and reservoir parameters can be learned by neural network. As shown in the top dotted box of Fig. 1, the predicted output of the network is compared with prepared label. We use the mean square error (MSE) as the loss function to measure the distance between the outputs and the labels.

2.2. Step 2: Re-training for application

When the pre-training step is completed, the trained network is retrained using the well log. The workflow is shown in the bottom box of

Table 1

Detailed parameters of our proposed A-Net architecture shown in Fig. 2.

Operation layer	Channel (Ic/Oc)	Kernel size (Ic × Oc × Ks)	Output size (Ih × Oc × Bs)
Input data	–	–	150 × 9 × 16
Conv1	9/11	9 × 11 × 3	150 × 11 × 16
Conv2	11/13	11 × 13 × 3	150 × 13 × 16
Conv3	13/15	13 × 15 × 3	150 × 15 × 16
Conv4	15/17	15 × 17 × 3	150 × 17 × 16
Conv5	17/19	17 × 19 × 3	150 × 19 × 16
Conv6	19/19	19 × 19 × 3	150 × 19 × 16
Conv5*	19/17	19 × 17 × 3	150 × 17 × 16
Conv4*	17/15	17 × 15 × 3	150 × 15 × 16
Conv3*	15/13	15 × 13 × 3	150 × 13 × 16
Conv2*	13/11	13 × 11 × 3	150 × 11 × 16
Conv1*	11/9	11 × 9 × 3	150 × 9 × 16
FC	1350 × 450	–	450 × 16
Output data	–	–	150 × 3 × 16

Fig. 1. When the two-step training of the network is completed, the network not only has the ability to map from pre-stack seismic data to reservoir parameters, but also has high resolution output due to the influence of well log data on the network. Finally, the reservoir parameters of the target data are inverted by the trained neural network.

Pre-stack seismic inversion is a regression problem that requires to make full use of the information in the training data, and the effect of learning is directly related to the scale of the network. Although the CNN can be applied to regression, and training CNN generally requires a large number of label data. The U-net does not have the requirement of abundant label, but it is mostly used for image segmentation problems (Ronneberger et al., 2015; Ibtehaz and RahmanSohel, 2020), and the role is to remove redundant information and extract high-dimensional feature. The structure with contracting path first and then expansive path is tend to remove weak information in seismic data, ignoring subtle differences between traces. Therefore, we design a fully redundant A-Net (Fig. 2), which first expanded the data to amplify weak information, and then compressed the path to extract key features. The main difference between A-net and U-net is that it enables full learning of

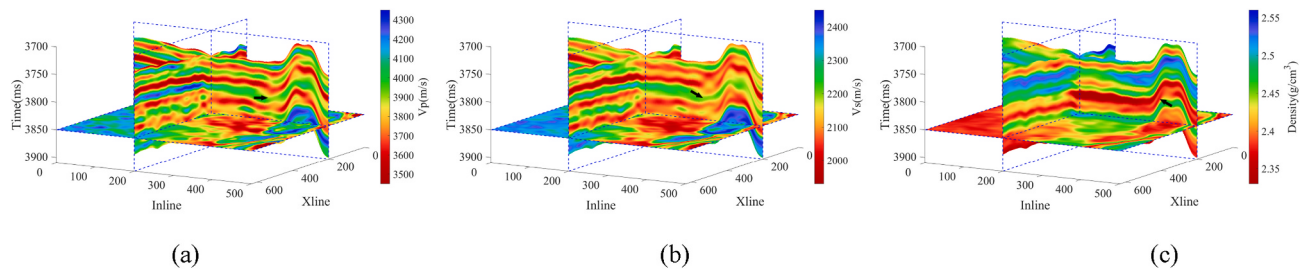


Fig. 6. The conventional inversion results of reservoir parameters. (a) V_p ; (b) V_s ; (c) ρ .

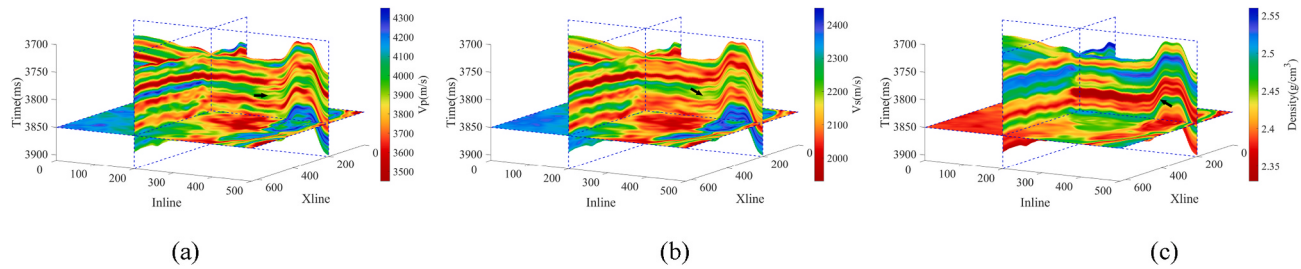


Fig. 7. The FSL high resolution inversion results of reservoir parameters. (a) V_p ; (b) V_s ; (c) ρ .

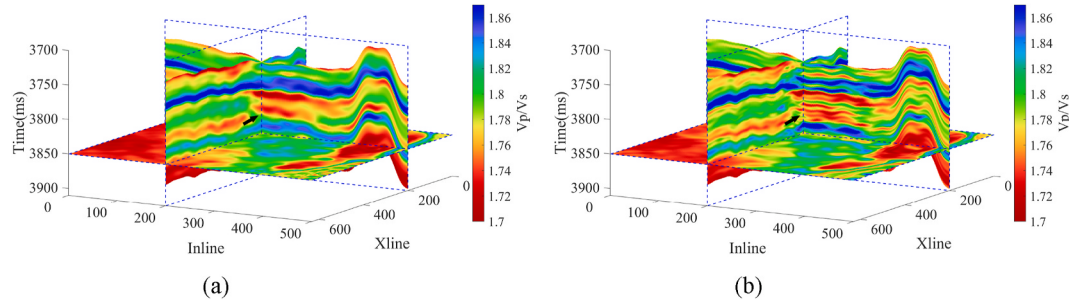


Fig. 8. The V_p/V_s of reservoir parameters. (a) The conventional inversion results; (b) The FSL-based high resolution inversion results.

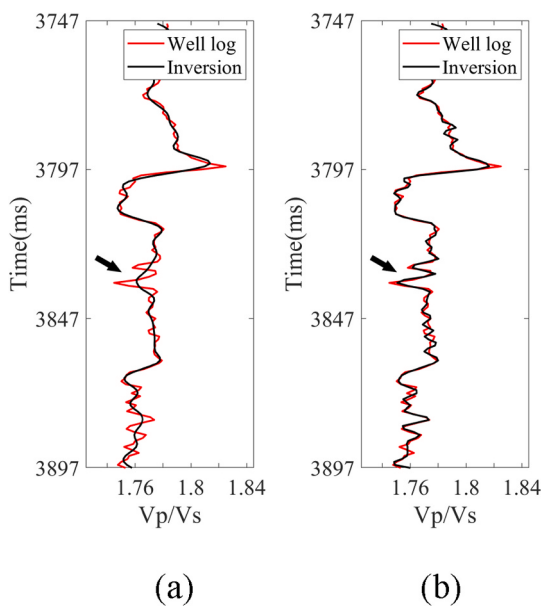


Fig. 9. The V_p/V_s of reservoir parameters. (a) The conventional inversion results; (b) The FSL-based high resolution inversion results.

redundant data, including subtle differences between data. Based on the learning capability of the A-net, we can get the desired reservoir parameters from pre-stack seismic data.

We used a PyTorch implement of 1D convolutional layer to build each convolutional unit (Fig. 3). At the end of each layers, we introduce the nonlinearity using normalized function (BatchNorm1d) and activation function (ReLU) defined as $\chi(\xi) = \max(0, \xi)$ (Nair and Hinton, 2010; Ioffe and Szegedy, 2015). There is also a linear mapping layer at the end of the network. It is found that scaling labeled data and the output of the network into a small range may accelerate the convergence process, especially with the Adam optimizer that provides “normalized” (i.e., the ratio of the first and the second momentum) parameter updates because all trainable parameters are randomly initialized in a range of [0,1]. Therefore, in experiments of this paper, the ground-truth reservoir parameters models are scaled using the global minimum and maximum of parameters values M_{min} and M_{max} , i.e., $(M - M_{min}) / (M_{max} - M_{min})$. To obtain the estimated reservoir parameters models, a reverse scaling procedure is required to assign each pixel of output into a parameters values, i.e., $M_{output} = M_{output} \times (M_{max} - M_{min}) + M_{min}$.

2.2.1. Example

We use a field dataset from the northwest of China to test the validity of the pre-stack inversion method based on FSL. This area features a lacustrine delta sedimentary environment with some large scale of interbedded sand-mudstone. The pre-stack data set covers a 100 km^2 area with $\text{inline}501 \times \text{xline}631 \times \text{angles}9$. There are 150 ms in each

trace with a sampling rate of 1 ms. The dominant frequency of seismic data is 40 Hz with an effective frequency band of 8–49 Hz. The target reservoir is TII0, a thin gas formation of Triassic located between the shore-shallow lake mudstone and the TII thick sandstone below. The distribution of lithology is inferred from GR and SP curves in well data. The shore-shallow lake mudstone formation is stable, and its thickness is about 30–48 m. TII0 gas formation has the characteristics of large buried depth (more than 4700 m) and uneven transverse distribution with the thickness is between 1 and 4.5 m. A mudstone intercalation between the TII0 and the lower TII sandstone has an uneven transverse of distribution thickness (3–8 m), locally thickness exceeding 10 m. Fig. 4 shows post-stack and angle-stack seismic data from near to far. The reservoir is sandstone with a small thickness and poor signal-noise ratio (SNR) of pre-stack 3D seismic data. As shown in Fig. 5, we display the proportion of lithology obtained from well log analysis. The yellow and gray coatings in the Figure represent the composition of sandstone to mudstone, respectively. The green curve is the GR log. The difference of P-impedance between sandstone and mudstone in TII0 is not obvious, but the sandstone has the characteristics of low V_p/V_s . Therefore, pre-stack inversion of V_p/V_s has the potential to identify reservoirs, and the reservoir can be distinguished in a small range.

The seismic data from each angles need to be normalized at the beginning, and then 2 wells are used to construct the initial low-frequency model for the conventional pre-stack inversion. The initial model of the well position is obtained by 12 Hz low-pass filtering of the well data, and then extrapolated to the remaining CDPs positions by interpolation. The 3D pre-stack inversion results of reservoir parameters based on low frequency constrained (Huck et al., 2010). Due to the poor quality of seismic data, conventional inversion results show low resolution, which cannot meet the needs of accurate reservoir identification.

For improving the resolution of reservoir parameters, we take the conventional inversion results as the auxiliary dataset for FSL inversion, while the scarce training dataset only has 16 valid well log. In addition to the well log used to construct the scarce dataset, one well that was not involved in the network training process was used as a blind well to test the effectiveness of the results. The auxiliary dataset is used to pre-train the network, and the scarce training dataset will re-train the network and adjust the weight of the network. We performed about 10 epochs to re-train the network. Detailed descriptions of A-net network parameters are presented in Table 1. Such as input channels (Ic), output channels (Oc), convolution kernel size (Ks), batch size (Bs), input data height (Ih).

After re-training, we use the trained network to predict V_p , V_s and ρ for the all CDPs positions in working area. It can be seen that retraining network with well log yields higher resolution results than conventional inversion, especially at the black arrow markers (Figs. 6 and 7). Fig. 8 shows the V_p/V_s constructed from the inversion results. The black arrow in Figs. 8 and 9 indicates the location of the target gas formation TII0. The inversion effect at this location in FSL-based inversion shows that the boundary between TII0 and surrounding mudstone is clear, and the thickness information of this formation can be accurately identified. We can see that the FSL-based inversion shows several thinner sandstone layers, while the conventional inversion shows a thicker sandstone response. A comprehensive comparison of the two methods inversion results shows that FSL-based inversion method can improve the resolution and accuracy of inversion results in pre-stack seismic inversion. Although the number of valid labeled data is small, the resolution of result is still acceptable. If the number of label is enough, we will get a better result.

3. Conclusion

In this paper, we propose a high resolution pre-stack seismic inversion method for reservoir parameters based on FSL. It contains a specially designed A-Net architecture. Through a field data example, we demonstrated the application of this network in resolving a high resolution pre-stack seismic inversion problem. The results show clear

improvement on the resolution of inversion results, which provides a reliable basis for the accurate identification of thin formation. The trade-off, however, is that this approach does require additional time cost and data dependency. Nevertheless, it can provide a solution for the insufficient sample in ANN inversion.

Declaration of competing interest

The authors declare that they have no known competing financial interests or personal relationships that could have appeared to influence the work reported in this paper.

Acknowledgment

We great appreciate the financial support from the National Natural Science Foundation of China (Grant No. 42130812, 42174151, and 41804126). We are grateful to the GeoSoftware for licensing the use of the Hampson-Russell software to us.

References

- Alemic, W., Sacchi, M.D., 2011. High-resolution three-term AVO inversion by means of a Trivariate Cauchy probability distribution. *Geophysics* 76 (3), R43–R55. <https://doi.org/10.1190/1.3554627>.
- Araya-Polo, M., Jennings, J., Adler, A., Dahlke, T., 2018. Deep-learning tomography. *Lead. Edge* 37 (1), 58–66. <https://doi.org/10.1190/tle37010058.1>.
- Biswas, R., Sen, M.K., Das, V., Mukerji, T., 2019. Pre-stack inversion using a physics-guided convolutional neural network. *SEG Technical Program Expanded Abstracts* 2019 4967–4971. <https://doi.org/10.1190/segam2019-3215071.1>.
- Chen, D., Gao, J., Hou, Y., Gao, Z., 2019. High resolution inversion of seismic wavelet and reflectivity using iterative deep neural networks. *SEG Technical Program Expanded Abstracts* 2019 2538–2542. <https://doi.org/10.1190/segam2019-3216178.1>.
- Dai, Y., Huang, X., Xu, Y., 2019. Seismic inversion based on deep learning and its impact by sample size. In: SEG 2019 Workshop: Fractured Reservoir & Unconventional Resources Forum: Prospects and Challenges in the Era of Big Data. Society of Exploration Geophysicists, pp. 65–68. https://doi.org/10.1190/frur2019_17.1. Lanzhou, China, 1–3 September 2019.
- Das, V., Pollack, A., Wollner, U., Mukerji, T., 2019. Convolutional neural network for seismic impedance inversion. *Geophysics* 84 (6), R869–R880. <https://doi.org/10.1190/geo2018-0838.1>.
- de Figueiredo, L.P., Grana, D., Roisenberg, M., Rodrigues, B.B., 2019. Gaussian mixture Markov chain Monte Carlo method for linear seismic inversion. *Geophysics* 84 (3), R463–R476. <https://doi.org/10.1190/geo2018-0529.1>.
- Goodfellow, I., Bengio, Y., Courville, A., 2016. Deep Learning. MIT press, Cambridge.
- Hampson, D.P., Russell, B.H., Bankhead, B., 2005. Simultaneous inversion of pre-stack seismic data. *SEG Technical Program Expanded Abstracts* 2005 1633–1637. <https://doi.org/10.1190/1.2148008>.
- Huck, A., Quiquerz, G., de Groot, P., 2010. Improving seismic inversion through detailed low frequency model building. In: 72nd EAGE Conference and Exhibition Incorporating SPE EUROPEC 2010. European Association of Geoscientists & Engineers, p. 161. <https://doi.org/10.3997/2214-4609.201400776>.
- Ibtehaz, Nabil, Rahman, M., Sohel, 2020. MultiResUNet: rethinking the U-Net architecture for multimodal biomedical image segmentation. *Neural Network* 121, 74–87. <https://doi.org/10.1016/j.neunet.2019.08.025>.
- Ioffe, S., Szegedy, C., 2015. Batch normalization: accelerating deep network training by reducing internal covariate shift. In: International Conference on Machine Learning, pp. 448–456.
- Krizhevsky, A., Sutskever, I., Hinton, G.E., 2012. Imagenet classification with deep convolutional neural networks. *Adv. Neural Inf. Process. Syst.* 25, 1097–1105.
- Lu, J., Gong, P., Ye, J., Zhang, C., 2020. Learning from Very Few Samples: A Survey arXiv preprint, arXiv: 2009.02653.
- Nair, V., Hinton, G.E., 2010. Rectified Linear Units Improve Restricted Boltzmann Machines. *ICML*.
- Richardson, A., 2018. Seismic Full-Waveform Inversion Using Deep Learning Tools and Techniques arXiv preprint, arXiv: 1801.07232.
- Ronneberger, O., Fischer, P., Brox, T., 2015. U-net: convolutional networks for biomedical image segmentation. In: International Conference on Medical Image Computing and Computer-Assisted Intervention, pp. 234–241. https://doi.org/10.1007/978-3-319-24574-4_28.
- Röth, G., Tarantola, A., 1994. Neural networks and inversion of seismic data. *J. Geophys. Res.* 99, 6753–6768. <https://doi.org/10.1029/93JB01563>.
- She, B., Wang, Y., Liang, J., Hu, G., 2019. Data-driven simultaneous seismic inversion of multiparameters via collaborative sparse representation. *Geophys. J. Int.* 218 (1), 313–332. <https://doi.org/10.1093/gji/ggz116>.
- Song, L., Yin, X., Zong, Z., Jiang, M., 2022. Semi-supervised learning seismic inversion based on Spatio-temporal sequence residual modeling neural network. *J. Petrol. Sci. Eng.* 208, 109549 <https://doi.org/10.1016/j.petrol.2021.109549>.

- Sun, J., Innanen, K.A., Huang, C., 2021. Physics-guided deep learning for seismic inversion with hybrid training and uncertainty analysis. *Geophysics* 86 (3), R303–R317. <https://doi.org/10.1190/geo2020-0312.1>.
- Zhang, J., Li, J., Chen, X., Li, Y., Huang, G., Chen, Y., 2021. Robust deep learning seismic inversion with a priori initial model constraint. *Geophys. J. Int.* 225 (3), 2001–2019. <https://doi.org/10.1093/gji/ggab074>.
- Zong, Z., Yin, X., Wu, G., 2012. AVO inversion and poroelasticity with P- and S-wave moduli. *Geophysics* 77, N17–N24. <https://doi.org/10.1190/geo2011-0214.1>.